2015-12-01

Identification of paleo Arctic winter sea ice limits and the marginal ice zone: Optimised biomarker-based reconstructions of late Quaternary Arctic sea ice

Belt, Simon

10.1016/j.epsl.2015.09.020
EARTH AND PLANETARY SCIENCE LETTERS
Elsevier BV

Identification of paleo Arctic winter sea ice limits and the marginal ice zone: optimised biomarker-based reconstructions of late Quaternary Arctic sea ice.

Simon T Belt[a,*],Patricia Cabedo-Sanz [a], Lukas Smik [a],Alba Navarro-Rodriguez [a], Sarah M P Berben[b,1],JochenKnies[c,d] and Katrine Husum [e]

(a) Biogeochemistry Research Centre, School of Geography, Earth and Environmental Sciences, Plymouth University, Plymouth, PL4 8AA, UK.

(b) Department of Geology, UiT – The Arctic University of Norway, N-9037 Tromsø, Norway

(c) Geological Survey of Norway, N-7491 Trondheim, Norway.

(d) CAGE - Centre for Arctic Gas Hydrate, Environment and Climate; Department of Geology, University of Tromsø, N-9037 Tromsø, Norway.

(e) Norwegian Polar Institute, Fram Centre, NO-9296 Tromsø, Norway.

* Author for correspondence

e-mail: sbelt@plymouth.ac.uk

Keywords: Sea ice; Arctic; Proxy; IP_{25}; Biomarker; Paleoclimate

[1] Current Address: Department of Earth Science and the Bjerknes Centre for Climate Research, University of Bergen, N-5007 Bergen, Norway.

Abstract

Analysis of >100 surface sediments from across the Barents Sea has shown that the relative abundances of the mono-unsaturated sea ice diatom-derived biomarker IP_{25} and a tri-unsaturated highly branched isoprenoid (HBI) lipid (HBI III) are characteristic of the overlying surface oceanographic conditions, most notably, the location of the seasonal sea ice edge. Thus, while IP_{25} is generally limited to locations experiencing seasonal sea ice, with higher abundances found for locations with longer periods of ice cover, HBI III is found in sediments from all sampling locations, but is significantly enhanced in sediments within the vicinity of the retreating sea ice edge or marginal ice zone (MIZ). The response of HBI III to this well-defined sea ice scenario also appears to be more selective than that of the more generic phytoplankton biomarker, brassicasterol. The potential for the combined analysis of IP_{25} and HBI III to provide more detailed assessments of past sea ice conditions than IP_{25} alone has been investigated by quantifying both biomarkers in three marine downcore records fromlocations with contrasting modern sea ice settings. For sediment cores from the western Barents Sea (intermittent seasonal sea ice) and the northern Norwegian Sea (ice-free), high IP_{25} and low HBI III during the Younger Dryas (ca. 12.9–11.9 cal. kyr BP) is consistent with extensive sea cover, with relatively short periods of ice-free conditions resulting from late summer retreat. Towards the end of the YD (ca. 11.9–11.5 cal. kyr BP), a general amelioration of conditions resulted in a near winter maximum ice edge scenario for both locations, although this was somewhat variable, and the eventual transition to predominantly ice-free conditions was later for the western Barents Sea site (ca. 9.9 cal. kyr BP) compared to NW

Norway (ca. 11.5 cal. kyr BP). For both locations, coeval elevated HBI III (but absent IP_{25}) potentially provides further evidence for increased Atlantic Water inflow during the early Holocene, but this interpretation requires further investigation. In contrast, IP_{25} and HBI III data obtained from a core from the northern Barents Sea demonstrate that seasonal sea ice prevailed throughout the Holocene, but with a gradual shift from winter ice edge conditions during the early Holocene to more sustained ice cover in the Neoglacial; a directional shift that has undergone a reverse in the last ca. 150 yr according to observational records. Our combined surface and downcore datasets suggest that combined analysis of IP_{25} and HBI III can provide information on temporal variations in the position of the maximum (winter) Arctic sea ice extent, together with insights into sea ice seasonality by characterisation of the MIZ.Combining IP_{25} with HBI III in the form of the previously proposed PIP_{25} index yields similar outcomes to those obtained using brassicasterol as the phytoplankton marker. Importantly, however, some problems associated with use of a variable balance factor employed in the PIP_{25} calculation, are potentially alleviated using HBI III.

1. Introduction

Sea ice plays a major role in controlling the energy budget at the Earth's surface by reflecting a significant part (>90%) of incoming radiation due to the so-called albedo effect. Sea ice also acts as a physical barrier to heat and gas exchange between the oceans and the atmosphere, and contributes to ocean circulation through brine release during formation and freshwater discharge during melting (e.g. Dickson et al., 2007 and references therein). It also experiences large seasonal variations and inter-annual variation can also be significant. Variations in sea ice also influence climate change scenarios beyond the polar regions through tele-connections (e.g. Wang et al., 2005). However, despite recognition of the key roles that sea ice plays in global climate, with recent reductions in extent and thickness attracting considerable attention (e.g. Stroeve et al., 2012), long term records of sea ice and variations in its distribution have, until recently, remained relatively scarce, principally due to a combination of the logistical constraints of working in the polar regions and a lack of suitable (proxy) methodologies. Observational records of past sea ice are spatially incomplete and, in any case, rarely extend beyond a few hundred years (Divine and Dick, 2006), while reconstructions based on geological archives areparticularly challenging since sea ice leaves no direct legacy signature in marine or terrestrial records; however, a number of proxy methods have been developed to specifically address this. Some of these approaches are based on the responses of pelagic or benthic organisms whose distributions and composition (e.g. stable isotopes) are influenced by sea ice cover (for an overview, see de Vernal et al., 2013 and references therein), while others rely on the identification of

material entrained within the sea ice itself (i.e. ice-rafted debris (IRD)) which is deposited in sediments following release from melting ice (Andrews, 2009).

In recent years, the analysis of the biomarker IP_{25} (structure I; Fig. 1; Belt et al., 2007), a C_{25}highly branched isoprenoid (HBI) lipid made uniquely by certain Arctic sea ice-dwelling diatoms (Brown et al., 2014), has been suggested to provide a more direct measure of past sea ice when detected in underlying sediments (see Belt and Müller, 2013 for a recent review). Importantly, IP_{25} has been identified in sediments from a large number of surface sediments from seasonally ice-covered Arctic locations and downcore records spanning timescales from recent decades (Müller et al., 2011; Stoynovaet al., 2013; Xiao et al., 2013; Navarro-Rodriguez et al., 2013), the Holocene (Vareet al., 2009; Müller et al., 2012) and even longer (Stein and Fahl, 2013; Knies et al., 2014; Müller and Stein, 2014). A remaining question, however, concerns the extent to which the analysis of IP_{25} can provide more detailed or quantitative estimates of paleo sea ice. Initially, Massé et al. (2008) demonstrated that IP_{25} abundances in a marine core from the North Icelandic Shelf exhibited a strong relationship to known sea ice conditions in observational records and, in general, changes in sedimentary concentrations of IP_{25} are consistent with corresponding variations in sea ice extent (Belt and Müller, 2013). Absolute abundances of IP_{25}, however, vary considerably between different Arctic regions with otherwise similar sea ice extent and no strict relationship with sea ice concentration exists. Despite this limitation, the selectivity of sedimentary IP_{25} to seasonally ice-covered locations largely remains, making its presence a useful qualitative sea ice proxy, at least.

Exceptionally, IP_{25} has been identified in a small number of sediments from either ice-free locations or those from near permanent ice cover, although these are likely explained by sediment advection and (at least) partial ice melt, respectively (Navarro-Rodriguez et al., 2013; Xiao et al., 2015).

In order to distinguish between the two extreme scenarios of ice-free conditions and permanent ice cover, more generally, Müller et al. (2009) suggested the parallel measurement of pelagic phytoplankton biomarkers that mightbe considered indicators of ice-free sea surface conditions. As such, the absence or low abundance of phytoplankton sterol lipids such as brassicasterol may serve to indicate permanent sea ice coverage, while elevated brassicasterol content would suggest predominantly ice-free conditions. The success of this approach inconstructing sea ice conditions for the Fram Strait over the last 30 kyr (Müller et al., 2009) led to the subsequent development of the so-called PIP_{25} index, whereby concentrations of IP_{25} and a phytoplankton biomarker (typically brassicasterol) are combined to provide semi-quantitative estimates of sea ice concentration (Müller et al.,2011).However, although relationships between PIP_{25} data and sea ice concentrations are, in general, better than those using IP_{25} alone (e.g. Xiao et al., 2015), this is not always the case (Navarro-Rodriguez et al., 2013) and the underlying reasons for such improved correlations are not fully resolved, not least due to the uncertainties in the true inter-relationshipbetween IP_{25} and phytoplankton lipids under different sea ice settings, or the strict pelagic origin of brassicasterol in all cases (e.g. Fahl and Stein, 2012; Belt et al., 2013; Xiao et al., 2015).

An alternative approach may be better focussedon improving our understanding of different sea ice *conditions* (e.g. seasonal ice, drift ice)rather than sea ice *concentrations*,especially if biological processes,and signatures of these, areparticularly characteristicof the former. Indeed, establishing parameters such as the winter/summer ice margins or sea ice seasonality are especially important since they are used as boundary parameters in climate forecasting and hindcasting models. In this respect, PIP_{25}data have also beeninterpreted in terms of categorisation of sea ice conditions (Müller et al., 2011) although further caveats also exist. Amongst its identified limitations (see Belt and Müller (2013) for a comprehensive review), the variable sources of brassicasterol and the potential lack of sensitivity of its production to individual environmental settings make reconstruction of different sea ice conditions rather challenging, for certain regions at least. For example, brassicasterol may have influences from pelagic, sea ice, freshwater and terrestrial input (Huang and Meinschein, 1976; Volkman, 1986;Fahl and Stein, 2012; Belt et al., 2013; Xiao et al., 2015), while abundances in Barents Sea surface sediments were not substantially different between seasonally ice-covered and year-round ice-free locations(Navarro-Rodriguez et al., 2013). A further issue, when using phytoplankton sterols as indicators of the open-water setting,concerns the so-called balance factor (*c*) used in the PIP_{25} calculation, and employed to accommodate the (generally) substantially higher sedimentary concentrations of sterols compared to IP_{25}. In particular, since the magnitude of *c* is dependent on both the number and nature of the samples from which it is derived, outcomes from surface calibrations and

downcore records may be modified dramatically, for example, simply on the basis of which sedimentary sections are being analysed. Recently, Xiao et al (2015) suggested that a global *c* factor might be more useful in this respect; however, the occurrence of significant regional differences emphasizes that selection of the most appropriate value remains problematic.

A related strategy conceivably involves the analysis of a different lipid biomarker that, like IP_{25}, has a well-defined or constrained source, whose production is more closely aligned with certain pelagic (or sea ice) conditions, and has sedimentary concentrations closer to those of IP_{25}, thus potentially removing the need to employ a balance factor when calculating PIP_{25} indices. In the current study, we apply this approach using a further C_{25} HBI lipid,which, like IP_{25}, is believed to be biosynthesised by a relatively small number of marine diatom genera yet, in contrast to IP_{25}, does not appear to be biosynthesised by sea ice diatoms or other sources. This tri-unsaturated HBI (HBI III; Fig. 1) is found commonly in marine sediments from temperate settings worldwide (Belt et al., 2000) and also in Antarctic phytoplankton and sediments (Massé et al., 2011). Indeed, HBI III has been further hypothesised to represent a potential proxy for the pelagic environment adjacent to retreating sea ice or the marginal ice zone (MIZ) in the Antarctic (Collins et al., 2013). Such a hypothesis was based on the similarities in temporal profiles within Scotia Sea sediments, of HBI III and a di-unsaturated HBI (HBI II; Fig. 1), considered to be a sea ice proxy in the Antarctic (Massé et al., 2011; Collins et al., 2013). However, the analyses of surface sediments or

194 phytoplankton from such locations to support this hypothesis further have not,
195 as yet, been presented.
196
197 Here, we analysed biomarker lipids (IP_{25}, HBI III and brassicasterol) in surface
198 and downcore sediment material from locations across the Barents Sea, in
199 part, because the region has a reasonably well-defined annual sea ice
200 advance/retreat cycle, and also since complementary observational and proxy
201 data were available. In addition, Vare et al. (2010) demonstrated that
202 abundances of IP_{25} in dated short cores from the region aligned well with
203 observational sea ice records covering the last few hundred years.
204 Comparison of our findings from surface sediments with those of downcore
205 records suggests that combined analysis of IP_{25} and HBI III can be used
206 tocharacterise the maximum (winter) sea ice extent and MIZ,in particular, thus
207 providing more detailed information regarding paleo sea ice conditions than
208 through analysis of IP_{25}(or PIP_{25}) alone.
209
210 **2. Regional setting**
211 The Barents Sea is a relatively shallow (mean depth 230 m) epicontinental
212 shelf between the north Norwegian coast and the Svalbard archipelago that
213 plays a crucial role in the Arctic climate system, largely, since it contributes to
214 significant heat exchange between the ocean and the atmosphere (Serreze et
215 al., 2007). Detailed descriptions of the main surface currents in the Barents
216 Sea (and the adjacent northern Norwegian Sea) can be found elsewhere
217 (Loeng, 1991) and a summary is shown in Fig. 2a. In brief, the North Atlantic
218 Current (NAC) delivers relatively warm salty Atlantic water (>2°C; >35‰;

Hopkins, 1991) into the northern North Atlantic (Swift, 1986) before dividing into the West Spitsbergen Current (WSC) and the North Cape Current (NCaC) which provide inflow to the Arctic Oceanand the Barents Sea, respectively, with a further branch of theNCaCflowing parallel with the coastal current system (Loeng, 1991).In contrast, colder and less saline Polar water (0-2°C; 33-34.4‰; Hopkins, 1991) is brought into the Atlantic Ocean from the Arctic Ocean by the East Greenland Current (EGC) and into the Barents Sea by the East Spitsbergen Current (ESC) and Bear Island Current (BIC). Polar and Atlantic water meet in the Barents Sea to form Arctic water (ca. 0.5°C; ca. 34.8‰; Hopkins, 1991), which is characterized by reduced temperature and salinity, as well as the occurrence of seasonal sea ice (Hopkins, 1991). Warm and fresh coastal water (2-13°C, 32-35‰; Hopkins, 1991) is found on the shelves and off the coast of Norway and is transported northwards by the Norwegian Coastal Current (NCC) into the South-West Barents Sea and along the Norwegian and Russian coastline (Aure and Strand, 2001).

Of particular significance to this region, the boundaries between Polar/Arctic and Arctic/Atlantic waters correspond to the Polar Front and Arctic Front, respectively, both of which represent a sharp climatic gradient in terms of temperature, salinity and sea ice coverage (Hopkins, 1991). The overall extent of sea ice distribution in the northern North Atlantic and the Barents Sea, therefore, is closely related to the positions of the Polar and Arctic Fronts, which represent the average summer and winter sea ice margins, respectively (Vinje, 1977). Consequently, sea ice is formed during autumn and winter in the north-eastern Barents Sea (Loeng, 1991), while the southern

Barents Sea is characterized by large seasonal and inter-annual sea ice distribution changes, largely due to the strong (and variable) influence of inflowing Atlantic Water (AW) (Kvingedal, 2005). Such changes in sea ice can be readily seen by the locations of the maximum, minimum and median April sea ice extent for the period 1980-2015 derived from satellite data (NSIDC; Fig. 3). A significant contribution to the annual primary production in the Barents Sea results from a peak algal bloom during the spring as ice retreats along the ice edge or MIZ (Sakshaug et al., 2009).

3. Material and methods

3.1. Surface sediment material

Surface sediment samples were collected and analysed from a broad range of locations within the Barents Sea (Fig. 2b) using box cores, multicores and gravity cores. The majority of the surface sediment samples (0–1 cm) have been described elsewhere (Navarro-Rodriguez et al., 2013) and these have been supplemented for the current study with additional samples from the MAREANO program (Knies and Martinez, 2009) and further material collected on-board the *James Clark Ross* (UK) and the *Polarstern* (Germany) research vessels during oceanographic cruises JR142 and ARK-VIII/2in 2006 and 1991, respectively. A summary of all core locations and biomarker data can be found in Supplementary Table 1.

3.2.Downcore sediment material

Descriptions of the marine sediment cores analysed for the temporal part of this study (including core chronologies) can also been foundin detail

elsewhere. Briefly, coreJM99-1200 was collected from the Andfjorden, northern Norway (69.16˚ N, 16.25˚ E)and is described in Ebbesen and Hald (2004), Knies (2005) and Cabedo-Sanz et al. (2013). Core NP05-11-70GC was retrieved from the Olga Basin, northern Barents Sea (78.40° N, 32.42° E) and has been described previously by Berben (2014). Finally, core JM09-KA11-GC was collected from the Kveithola Trough, western Barents Sea (74.87° N; 16.48° E),and details can be found inRüther et al. (2012) and Berben et al., (2014).The age model for JM09-KA11-GCused in Berben et al. (2014) has been supplemented using a further ^{14}C date (ca. 13.12 cal. kyr BP; Rüther et al., 2012) in order for us to be able to extend the biomarker record to cover the Younger Dryas (YD). Hereafter, cores JM99-1200, NP05-11-70GC and JM09-KA11-GC are referred to as 1200, 70 and 11, respectively.

3.3. Biomarker analyses

Details of the extraction and analysis of HBI and sterol lipids described herein can be found elsewhere (Belt et al., 2012, 2013). Briefly, ca. 1–5 g of freeze dried sediment material was extracted (dichloromethane/methanol; 3 x 3 mL; 2:1 v/v) by ultrasonication following addition of internal standards (9-octylheptadec-8-ene (10 µL; 1 µg mL^{-1}) and 5α-androstan-3β-ol (10 µL; 1 µg mL^{-1}) for the quantification of HBI lipids andbrassicasterol, respectively. Where necessary, elemental sulfur was removed from the resulting total organic extracts (TOEs)(Cabedo-Sanz and Belt, 2015) and thesepartially purified TOEs were then separated into fractions containing HBIs and sterols as described previously (e.g. Belt et al., 2012). Fractions containing brassicasterol were derivatized using N,O-Bis(trimethylsilyl)trifluoroacetamide

294 (BSTFA, 50 µL, 70 °C; 1h).All fractions were analysed using gas
295 chromatography–mass spectrometry (GC–MS) with operating conditions as
296 described by Belt et al. (2012). Identification of individual lipids was based on
297 their characteristic GC retention times and mass spectra compared with those
298 of reference compounds, while quantification was achieved by comparison of
299 peak area integrations of selected ions (*m*/*z* 350 (IP_{25}); 346 (HBI III); 470
300 (brassicasterol)) with those of the internal standard in selected ion monitoring
301 (SIM) mode (Belt et al., 2012). These ratios were normalized to instrumental
302 response factors obtained for individual lipids and sediment mass (Belt et al.,
303 2012).Our data comprise some previously reportedconcentrationsof IP_{25} and
304 brassicasterol in surface sediments from the Barents Sea (Navarro-Rodriguez
305 et al., 2013) and these have been supplemented by some new data obtained
306 as part of the current study. All of the HBI III concentration data are new to
307 this study. We have also confined our dataset to those locations for which we
308 have IP_{25} and HBI III concentrations data, at least, and all three biomarkers
309 for the majority of locations. Exceptionally, brassicasterol was not measured
310 in a small number of surface sediments from NW Norway. PIP_{25} values were
311 calculated using the formula $PIP_{25} = IP_{25}/(IP_{25}+cP)$, with individual terms as
312 described by Müller et al. (2011).Two-tailed t-tests were performed and
313 interpreted (95% confidence limits) for statistical analyses.
314
315 *3.4. Sea ice data*
316 In order to place ourbiomarker data into a spatial and recent temporal sea ice
317 context, we obtained estimates of sea ice extent using polyline shapefiles
318 derived from satellite data collectedfor the period 1981-2010 (NSIDC). From

these, we identified the individual years of (overall) maximum and minimum extent for April (winter maximum), and the median positionsof the maximum (April) and minimum (September)ice edge. Thisinterval is suitable for contextualising surface (typically 0–1 cm) sediment data since accumulation rates in the region are generally of the order of 1 cm yr^{-1} (Maitiet al., 2010; Vare et al., 2010).

4. Results and discussion

4.1. Biomarkers in surface sediments – characterisation of the winter ice edge and the MIZ

In total, 102 surface sediment samples were analysed for $IP_{25}$and HBI III. Of these, 75 were also analysed for brassicasterol. Consistent with previous findings, the sea ice biomarker IP_{25} was identified in 44 out of 45 (98%) extracts obtained from seasonally ice-covered locations (Fig. 3a). Exceptionally, IP_{25} was also identified in a few (7 out of 57; 13%) sediments from locations south of the maximum winter sea ice extent and this has been attributed, previously, to some likely allochthonous input or sediment advection from locations further up the slope (Navarro-Rodriguez et al., 2013) rather than local (autochthonous) production. In addition, the mean IP_{25} concentration for locations further north of the median April sea ice edge, with ice also persisting past June(5.5±3.3 ng g^{-1}; n=22), was significantly higher (p=0.01)than for locations proximal to the winter sea ice edge (3.1±2.5 ng g^{-1}; n=23). We interpret these findings as indicating enhanced IP_{25} production

(and subsequent deposition) for areas experiencing longer seasonal sea ice cover,with melt only occurring during late summer, while lower sedimentary IP_{25} abundances are found for locations that do not always experience sea ice cover on an annual basis and where spring-summer ice retreat occurs earlier (e.g. May–June).Consistent with this difference, IP_{25} is normally absent (or below the limit of detection) for the majority of locations beyond the maximum winter sea ice margin.

Some quite different trends are apparentfrom the HBI III data, however. For example, in contrast to IP_{25}, HBI III was present in virtually all (101 out of 102; 99%) of the sediment extracts, consistent with a pelagic phytoplankticorigin for this biomarker rather than sea ice diatoms. Indeed, as far as we are aware, HBI III has, to date, not been identified in Arctic sea ice.Concentrations of HBI III wererelativelylow for regions that experience annual and extensive sea ice cover (mean 0.40±0.38 ng g^{-1}; Fig 3b), whichcontrasts the enhanced IP_{25} abundances for the same locations (Fig. 3a), likely as a consequence of shorter (and cooler) summer seasons with lower phytoplankton productivity (Sakshaug et al., 2009).A somewhathigher mean HBI III concentration (1.7±1.6 ng g^{-1}; n=57)wasfound for ice-free locations in the southern (and warmer) region of samplingconsistent with increased productivity in this region (Sakshauget al., 2009). When compared against both of these two regions, however, asignificantly higher($p<0.001$) mean HBI III concentration (13.0±8.3 ng g^{-1}; n=23)was observed for locations bordered by the minimum (2006) and maximum (1981) April ice margins (Fig. 3b). The enhancement of HBI III in this region, especially relative to locations further north, represents a clear

reversal intrend compared to IP_{25}, and suggestsincreased production during late spring/early summer, which is reduced for locations with longer lasting sea ice cover. However, it is also evident that the mean HBI III concentration for this region of retreating ice edge is substantially (ca. 7–8 times) higher than for the annually ice-free locations, and is thus indicative of the well-known enhanced phytoplankton production within the MIZ as sea ice retreats during late spring (April-May) and into early summer (June) (Sakshauget al., 2009).

In order to assess whether the trends observed for HBI III could be identified through other pelagic productivity indicators, we considered the distribution pattern for the phytoplankton marker brassicasterol (Fig. 3c). In accord with the trends identified for HBI III, the mean brassicasterol concentration was lowest for the region with most persistent sea ice cover (375±177 ng g^{-1}; n=22), slightly higher for ice-free settings (695±1200 ng g^{-1}; n=33), and highest for locations within the MIZ (1470±1200 ng g^{-1}; n=20). However, the relative changes between the three regions were clearly greater for HBI III than for brassicasterol. Most noticeably, the mean enhancement of HBI III between the MIZ and the region with more extended seasonal ice cover (x32.5) was more than eight times that of brassicasterol (x3.9), probablybecause the latter is a common component in marine phytoplankton and its distribution pattern reflects productivity spanning all growth seasons, while the former is likely biosynthesised by a much smaller number of sources, but whose growth is especially favoured by, or at least more tolerant to, the nutrient-rich and stratified upper water column found at the ice-edge.

394 The differences in distribution of brassicasterol between regions may be
395 further complicated or blurred by production of this sterol in certain sea ice
396 diatoms (e.g. Belt et al., 2013)and other sources (Volkman, 1986), especially
397 for locations that may receive contributions from terrestrial sources (Huang
398 and Meinschein, 1976; Volkman, 1986; Fahl and Stein, 2012; Xiao et al.,
399 2015). In contrast, although the exact sources of HBI III in the study region
400 have not been firmly identified, the only known producers of this biomarkerare
401 marine diatoms within the genera *Pleurosigma*(Belt et al., 2000) and
402 *Rhizosolenia*(Rowland et al., 2001). Further, when measured in Arctic marine
403 sediments, HBI III has a stable isotopic composition ($\delta^{13}C$ ca. -35 to -40 ‰;
404 Belt et al., 2008) consistent with a polar phytoplanktic origin (Massé et al.,
405 2011) where cold and CO_2-enriched waters can result in highly depleted ^{13}C
406 composition (Tolosa et al., 2013).
407
408 In summary, our surface sediment data reinforce the view that the biomarker
409 IP_{25} has a highly selective sea ice diatom origin, with sedimentary
410 abundances enhanced for regions experiencing more frequent and longer-
411 lasting spring sea ice cover. In contrast, HBI III is common to all seasonally
412 ice-free regions, but is especially enhanced in sediments for locations that
413 reflect the retreating ice edge or MIZ during late spring-summer. Such
414 observations are likely driven by the individual diatom genera responsible for
415 the biosynthesis of IP_{25} and HBI III, while the distinctive differences in their
416 stable isotopic composition confirms the contrasting environments in which
417 they are produced.
418

4.2 Temporal biomarker profiles and identification of sea ice conditions

In order to establish whether the dataand outcomes from the surface sediment analyses could be used to provide more detailed descriptions of sea ice conditions over longer timescales, we analysed IP_{25}, HBI III and brassicasterolin three well-dated marine sequences from locations with contrasting modern sea ice cover (*viz*.long-lasting seasonal ice, inter-annual ice edge, ice-free) and compared outcomes with our surface sediment data and previous findings.

4.2.1. Olga Basin (northern Barents Sea)

Core 70 was retrieved from the Olga Basin in the northern Barents Sea, a location that, in modern times, experiences annual sea ice cover that forms during autumn/winter. Ice retreat occurs during the summer such that the site is normally only ice-free during August and September (Fig. 2b). Our biomarker record for core 70 covers the last ca. 9.5 cal. kyr BP. IP_{25} concentration (Fig. 4a) is low during the early part of the record and increases steadily towards recent times, with a core-top value similar to that found in nearby surface sediments (Navarro-Rodriguez, 2014). Anopposite trend is observed for HBI III (Fig. 4b), however, with highest concentrations occurring in the early Holocene and a decline towards the recent record, where values (ca. 1 ng g^{-1}) are also within the range found for nearby surface sediments (ca. 0.1–1.6 ng g^{-1}; Fig. 3b). A small decline in the brassicasterol concentration is also observed (Fig. 4c), but this is not as pronounced as for HBI III, possibly due to a lower sensitivity to the overlying sea ice conditions as demonstrated through our surface sediment data.

Previously, Berben (2014)suggested that these IP_{25} and brassicasterol data indicated seasonal sea ice cover throughout the record, but with shorter spring sea ice cover and longer (and warmer) summers during the early Holocene. These conclusions were supported further by the species distribution, preservation state and isotopic composition of planktic foraminifera. Berben (2014) also hypothesisedthat the position of the winter/spring ice-edge was in the proximity of the core 70 site during the early Holocene before advancing south and towards the modern sea ice limit after ca. 6.5cal. kyr BP. Significantly, therefore, we observe elevated HBI III during the early Holocene (ca. 9.5–8.5 cal. kyr BP), during which time, the mean concentration (ca. 11 ng g^{-1}) resemblesthat found for the modern sea ice edge locations (13.0 ng g^{-1}). At the same time, lower (compared to modern) IP_{25} concentrations arealso consistent with a modern winter/spring scenario. As such, the combined IP_{25} and HBI III data for core70 in the early Holocene reflect sea ice edge conditions normallyassociated with locations further south during modern times. Similarly, by consideration of the contrasting responses between IP_{25} and HBI III in surface sediments, together with the reversal in temporal profiles for IP_{25} and HBI III, we confirm agradual lengthening in seasonal ice durationover the core location throughout the Holocene (Berben, 2014), with progressivelyshorter (and cooler) summer seasons.

4.2.2.Kveithola Trough (western Barents Sea)

In contrast to the Olga Basin site, core 11 was obtained from a locationin the western Barents Sea close to the modern maximum winter sea ice extent and

thus experiences variable sea ice cover (presence/absence) on an annual basis and, in any case, for shorter periods (e.g. November–April). Consistent with such differences, IP_{25} concentrations in surface sediments from the western Barents Sea are much lower than those for the northern Barents Sea (Fig. 3a). Previously, Berben et al. (2014) reported relatively low abundances of IP_{25} in core 11 throughout the Holocene, although slightly elevated values were noted for the last ca. 1.0 cal.kyr BP, consistent with late Holocene increases in spring sea ice extent. However, relatively high IP_{25} and brassicasterol abundances were noted during the interval ca. 10.8–10.3 cal. kyr BP, while even higher IP_{25}(but lower brassicasterol) concentrations were observed in the earliest part of the record (ca. 11.9–10.8 cal. kyr BP). These were interpreted as reflecting, respectively, stable MIZ conditions (favourable for both biomarkers) during the early Holocene,which was preceded by a period of more extensive sea ice cover during the latter stages of the YD. Our data here extend those of Berben at al. (2014),withnew IP_{25} data for the YD (to ca. 13.0 cal. kyr BP),and HBI III concentrations for the entire record, thus providingeither clarification or further detail to these previous interpretations (Fig. 5). For example, during the majority of the YD (ca. 13 – 11.9 cal. kyr BP), IP_{25} concentrations are at their highest values throughout the entire record, after which, a reduction is observedbeginning ca. 11.9 calkyr BP, before reaching consistently lower levels ca. 11.3 cal. kyr BP (Fig. 5a). The elevated IP_{25} concentration during the YD is accompanied by extremely low HBI III abundance which, according to our surface datasets, is indicative ofconsistently long seasonal sea ice covercharacteristic of the northern Barents Sea in modern times (Figs. 3a, 3b). In contrast, lower IP_{25} and

494 intermittently higher HBI III concentrations can be seen for the period ca.
495 11.5–9.9 cal. yr BP, signifying stable ice edge or MIZ conditions. However, the
496 variability in the HBI III abundance, in particular, suggests that such winter ice
497 edge conditions probably did not prevail throughout the entire interval but
498 were more intermittent, with relatively frequent short-term changes compared
499 to the northern Barents Sea (core 70). Indeed, large temperature shifts have
500 beenrecorded previously for the western Barents Sea during this
501 interval,consistent with a high degree of climatic variability(Hald et al., 2007).
502 Our data suggest, therefore, that the most severe sea ice conditions for this
503 site only existed during the YD, with reasonably similar-to-modern conditions
504 reached by the early Holocene, whereupon they remained reasonably
505 consistent. Thus, for the majority of the Holocene sections after ca. 7.8 cal. yr
506 BP, IP_{25} was either very low in concentration or absent (Fig. 5a), while the
507 abundance of HBI III (Fig. 5b) was also lower than that observed in the
508 aforementioned intervals and similar to those seen for surface sediments from
509 ice-free locations further south (Figs. 3a, 3b), indicating only infrequent sea
510 ice cover at the core location. Exceptionally, during the early Holocene (ca.
511 9.9–7.8 cal. kyr BP), absent IP_{25} (or below our limit of detection) is
512 accompanied by relatively high HBI III concentrations, although this is not the
513 case for brassicasterol(see Section 4.2.5 for a discussion of this observation).
514 For this core, reduced brassicasterol during the YD followed by elevated
515 levels ca. 11.5–9.9 calkyr BP (Fig. 5c) also support the notion of a transition
516 from long seasonal ice cover to ice-edge conditions; however, there are also
517 some out-of-phase changes within the brassicasterol and HBI III profiles

during this interval, likely further reflecting the reduced selectivity of the formerand input from a range of sources.

4.2.3.Andfjorden (northern Norwegian Sea)

Our third case study (core 1200) represents a location in the northern Norwegian Sea and is thus significantly further south of the modern winter sea ice edge (Fig. 2). Not surprisingly, therefore, $IP_{25}$is absent in all surface sediments from nearby locations along the NW Norwegian coast (Fig. 3a). However, in a previous study, Cabedo-Sanz et al. (2013) demonstrated that the site was covered by extensive seasonal sea ice during the YD through identification of elevated IP_{25} levels between ca. 12.9–11.9 cal.kyr BP, but was ice-free (IP_{25} absent) throughout the early-mid Holocene (ca. 11.5–6.3 cal. kyr BP). During the termination of the YD (ca. 11.9–11.5 cal.kyr BP), significantly lower IP_{25} abundance compared to the previous millennium washypothesised to reflect reduced/more variable sea ice conditionsor shorter seasonal sea ice cover, but this was not investigated further. Here, we show that, consistent with the conclusions of Cabedo-Sanz et al. (2013) and our observations for core 11 (western Barents Sea), HBI III concentrations (Fig. 6b) are extremely low throughout the interval of elevated IP_{25} abundances during the YD (ca. 12.9–11.9 cal.kyr BP), indicativeof extensive sea ice extent associated with harsh winters and only short (ice-free) summers. Such conclusions are also in-line with low SST (Ebbesen and Hald, 2004) and other biogenic proxy data (Knies, 2005) obtained from the same core. Interestingly, during the subsequent period, with lower IP_{25}, HBI III concentrations increase markedly, albeit with some fluctuations in absolute values, including a zero

value at ca. 11.75 cal. kyr BP, coeval with absent IP_{25} and brassicasterol (Fig. 6), and interpreted previously as a short interval of extreme climate with permanent ice cover (Cabedo-Sanz et al., 2013). In general, however, we interpret this switch in relative abundances of IP_{25} and HBI III to indicate a transition from extensive sea ice cover,with only short intervals of ice-free cover during summers, from ca. 12.9–11.9 cal.kyr BP, to one of a (variable) winter ice edge scenario over the core location (and progressive retreat from this) from 11.9–11.5 cal.kyr BP, similar to what we propose for the western Barents Sea (core 11). This represents a modification to the interpretation of PIP_{25} data derived from core 1200 described previously (Cabedo-Sanz et al., 2013), where MIZ conditions were indicated for the majority of the YD (ca. 12.9–11.9 cal.kyr BP). However, PIP_{25} values (and the interpretations thereof) can be subject to considerable variability, especially as a consequence of changes to the balance factor, whose magnitude can be strongly influenced by thetemporal range of the core intervals being considered (see Introduction, section 4.2.4 and Belt and Müller, 2013). In addition, the brassicasterol data for core 1200do not reveal such clearly contrasting sea ice conditions as IP_{25} and HBI III, with alternating high and low abundances throughout the YD (Fig. 6c), likely reflecting the variable sources of this biomarker. Finally, and again consistent with observations made for 11, there is a period (ca. 11.5–9.2 cal. kyr BP) following the disappearance of IP_{25} from the record where HBI III concentrations are relatively high, but this is not evident in the brassicasterol profile (Fig. 6). The same combination of absent IP_{25}/high HBI III is also evident between ca.14.0–12.9 cal. kyr BP.

In summary, for each of cores 70, 11 and 1200, and for intervals where there is proxy evidence for past seasonal sea ice occurrence (i.e. IP_{25} present), the relative abundances and directional changes of IP_{25} and HBI III generally oppose each other, suggesting that the observations made for these biomarkers from surface sediments underlying contrasting seasonal sea ice extent in the Barents Seaare replicated in downcore records.In contrast, less consistent trends are observed between IP_{25} and brassicasterol profiles, probably as a result of the lower sensitivity of the latter to the overlying sea ice conditions, together with likely input from other (e.g. terrestrial) sources.

4.2.4. *Comparison of PIP_{25} indices using brassicasterol and HBI III as phytoplankton lipids*

In addition to establishing (and interpreting) the individual biomarker profiles, we also calculated PIP_{25} indices for each of our downcore records using brassicasterol and HBI III as the phytoplankton components (hereafter referred to as P_BIP_{25} and $P_{III}P_{25}$, respectively).In doing so, we chose to focus on the consistency (or otherwise) in outcomes using each biomarker and, more specifically, the impact of the balance factor *c*. Thus, for each of cores 70, 11 and 1200, PIP_{25} data were calculated using the method of Müller et al. (2011), whereby mean sedimentary concentrations of IP_{25} and the respective phytoplankton biomarker were used to determine core-specific *c* values, and complementary datasets, without using this term (i.e. c=1).

In all cases, application of the former approach yields similar outcomes when using either brassicasterol or HBI IIIas the phytoplankton marker with, for example, highest PIP_{25} values during the YD in cores 11 and 1200 (Fig. 5,6), consistent with the interval of most extensive sea ice cover, and increasing PIP_{25} values through the Holocene in core 70 (Fig. 4); such observations align well with the conclusions based on the individual biomarker profiles. A quite different picture emerges when PIP_{25} data are calculated for*c*=1, however. In particular, a dramatic shift (reduction) in P_BIP_{25} values is evident for all three cores (Fig. 4-6), yetthere are only very minor changesto the $P_{III}IP_{25}$ data. The impact of such substantial (*c*-influenced) changes in P_BIP_{25} values, and therefore in their interpretation, is illustrated particularly well in the case of core 70, where core-top P_BIP_{25} values range from ca. 0.9 using the derived *c* factor, to <0.1 for *c*=1 (Fig. 4), while the corresponding $P_{III}IP_{25}$ values are both ca. 0.9, and also consistent with modern conditions (i.e. extensive sea ice cover) according to the PIP_{25} categorisations of Müller et al. (2011). Of course, calculation of P_BIP_{25} using*c*=1may be considered a somewhat unrealistic scenario, especially if brassicasterol concentrations are always substantially higher than those of IP_{25}. In practice, however, this is not always true and, in some sediments, IP_{25} concentrations even exceed those of brassicasterol (e.g. Belt et al., 2013). In any case, these examples illustrates the impact that variable *c*can have on derived PIP_{25} data.In contrast, on the basis of the data presented here, use of HBI III for PIP_{25}-based sea ice estimates provides the same general outcomes to those obtained from some sterol-based values, but without the complications associated with a variable *c* factor. Determining the extent to which such an improvement on previous

617 approaches is more generally applicable, however, will require analysis of
618 downcore records from other regions and surface sediment-based
619 calibrations.
620
621 *4.2.5.Early Holocene anomalies – enhanced Atlantic Water inflow?*
622
623 For cores 11 and 1200, there are intervals during the early Holocene for which
624 IP_{25} is absent, but where levels of HBI III arerelatively high, before declining
625 and remaining low for the remainder of the records. Specifically, elevated HBI
626 III (but absent IP_{25}) occurred ca. 9.9–8.0 cal. kyr BP and ca. 11.2–9.3 cal. kyr
627 BP in cores 11 and 1200, respectively (Figs. 5, 6).This combination of IP_{25}
628 and HBI III does not occur for the northern Barents Sea site (core 70), since
629 IP_{25} is present throughout the record (Fig. 4a). Of course, the occurrence of
630 HBI III (but not IP_{25}) is not unexpected given the ubiquity of this biomarker in
631 surface sediments from across the study region, but the elevated abundances
632 compared to modern values represents something of an anomaly and
633 requires an attempt at explanation. At this stage, since the exact sources (and
634 depth habitats) of HBI III are not known, it is not possible to conclude with
635 certainty whether its occurrence reflects near-surface or sub-surface
636 conditions, especially as the likely diatom sources inhabit a dynamic range
637 across the photic zone. Potentially, therefore, enhanced HBI III during the
638 early Holocene could be explained by increased surface layer productivity
639 during the Holocene Thermal Maximum (HTM). However, since the HTM for
640 the Nordic/Barents Seas is believed to have occurred ca. 9.0–6.0kyr BP
641 (summarised by Risebrobakken et al., 2011), this explanation seems unlikely.

Alternatively, increased HBI III levels may better reflect the consequences of increased Atlantic Water inflow (with associated enhanced productivity) to the northern Norwegian Sea and Barents Sea, established as occurring ca. 10.0±1.0kyr BP (Risebrobakken et al., 2011). We note that elevated HBI III concentrations (but absent IP_{25}) also occur in core 1200 during the Allerød (ca. 13.8–12.9 cal. kyr BP; Fig. 6). Previously, Cabedo-Sanz et al. (2013) interpreted absent IP_{25} during this interval as indicative of ice-free conditions at this time, although an alternative explanation involving glacial re-advance could not be discounted. Our new HBI III data are not at all consistent with this latter hypothesis, however, so we conclude that ice-free conditions must have prevailed during this warm interval, with environmental conditions probably similar to those from ca. 11.5–9.2cal. kyr BP.

Determination of the sources (and major environmental habitats) of HBI III is clearly important, therefore, before elevated abundances of this biomarker can be interpreted fully, but we suggest thatquantification of this biomarker has the potential to add to the existing proxies used to probe climatic and oceanographic shifts in the Norwegian and Barents Seas, especially when measured alongside the sea ice biomarker proxy IP_{25}.

5. Conclusions

Analysis of >100 surface sediments from diverse regions across the Barents Sea has shown that the relative abundances of the diatom-derived biomarkers IP_{25} and HBI III are strongly dependent on the overlying oceanographic conditions, with the position of the seasonal sea ice edge playing a major role.

These observations are consistent with production of these biomarkers from source-specific diatoms, whose habitats are strongly dependent on the occurrence of seasonal sea ice. Thus, IP_{25} appears to be produced, selectively, by a small number of Arctic sea ice diatom species, while HBI III is made by other diatom species, whose habitat preference appears to be adjacent to the retreating sea ice edge. The potential for the combined analysis of IP_{25} and HBI III to provide more detailed assessments of past sea ice conditions has been tested by their quantification in three downcore records representing contrasting modern settings. The outcomes are not only consistent with previous general findings, but have allowed more detailed descriptions of sea conditions to be deciphered. Thus, for cores 11 and 1200, high IP_{25} and low HBI III during the YD are consistent with extensive sea cover, with relatively short periods of ice-free conditions resulting from late summer retreat. Towards the end of the YD (ca. 11.9 cal. kyr BP), a general amelioration of conditions resulted in a near winter maximum ice edge scenario, although this was somewhat variable and the eventualtransition to predominantly ice-free conditions was later for the western Barents Sea site (core 11; ca. 9.9 cal. kyr BP) compared to NW Norway (core 1200; ca. 11.5 cal. kyr BP), likely as a result of its more northerly location. In contrast, the northern Barents Sea site (core 70) was characterised by seasonal sea ice cover throughout the Holocene with a gradual shift from winter ice edge conditions during the early Holocene to more sustained ice cover in the Neoglacial; a transition that has undergone something of a reverse in the last ca. 150 yr according to observational records (Divine and Dick, 2006).

692 Our next objective will be to carry out a more detailed investigation into the
693 combined use of IP_{25} and HBI III in some form of numerical index (e.g. PIP_{25})
694 to ascertain whether more quantitative estimates of sea ice concentration are
695 achievable. For now, we note that surface $P_{III}IP_{25}$ values of 0.85 and <0.1 in
696 cores 70 and 11, respectively, are in excellent agreement with the
697 corresponding modern spring sea ice concentrations of ca. 80 and 5% (mean
698 1981-2010; NSIDC) for these two locations.
699
700 In the future, it will also be important to examine relative abundances of IP_{25}
701 and HBI III in surface and downcore records from other Arctic (and temperate)
702 regions to determine the wider applicability of this approach for detailed paleo
703 sea ice reconstruction. In this respect, we note that IP_{25} has been reported in
704 sediments from a wide range of Arctic locations (Belt and Müller, 2013; Brown
705 et al., 2014), while HBI III is one of the most frequently occurring HBIs found
706 in marine sediments worldwide (Belt et al., 2000), likely as a result of
707 production by common diatom genera (*Pleurosigma* and *Rhizosolenia*). We
708 also note that the enhanced primary production that is characteristic of the
709 retreating sea ice edge, and identified here through the proxy biomarker HBI
710 III, is a common feature within MIZ regions across the Arctic (Perette et al.,
711 2011).
712
713 In summary, our primary aim here was to investigate the potential for selected
714 biomarkers to provide complementary (at least) information to the qualitative
715 (IP_{25}) and semi-quantitative (PIP_{25}) methods established previously. To place

716 our findings within this broader context, we propose the following assessment
717 of the current status of biomarker-based (Arctic) sea ice proxies:
718
719 1. The occurrence of IP_{25} in Arctic marine sediments represents a highly
720 selective indicator of the past occurrence of seasonal sea ice cover,
721 spanning timeframes as far back as the late Pliocene (at least).
722 2. Substantial regional variability, in particular, means that algorithmic
723 relationships between sedimentary IP_{25}abundance and seasonal sea
724 ice concentration are not particularly reliable; however, higher
725 IP_{25}abundances are generally associated with enhanced sea ice extent
726 and downcore records are internally consistent (i.e. they reflect
727 directional changes in sea ice extent).
728 3. Semi-quantitative estimates of spring sea ice *concentration* may be
729 improved by combining IP_{25} with other biomarkers such as those
730 biosynthesised by open-water phytoplankton; however, issues
731 regarding regional versus global calibrations still need resolving, while
732 the limitations of using a variable balance factor in calculating PIP_{25}
733 indices is particularly problematic.
734 4. More accurate descriptions of spring sea ice *conditions* are achievable
735 by measuring IP_{25} alongside other source-specific biomarkers (e.g. HBI
736 III) whose production is particularly reflective of the neighbouring sea
737 ice conditions (e.g. winter sea ice margin, marginal ice zone) as shown
738 in the current study. The potential for using such a marker for more
739 semi-quantitative sea ice estimates using the PIP_{25} (or related) index is

740 especially attractive, not least, since problems associated with using a
741 variable balance factor may be alleviated.
742
743
744 **Acknowledgments**
745 This work is a contribution to the CASE Initial Training Network funded by the
746 European Community's 7th Framework Programme FP7 2007/2013, Marie-
747 Curie Actions, under Grant Agreement No. 238111. We also thank Professor
748 Ruediger Stein (AWI) and The British Ocean Sediment Core Research Facility
749 (BOSCORF)for providing us with some of the surface sediment material (PS
750 and JR142 samples, respectively) described in this study and we are also
751 grateful to Shaun Lewin (Plymouth University) for assistance with the
752 cartography. We thank three anonymous reviewers for providing supportive
753 feedback and helpful suggestions to improve the manuscript.
754
755
756
757
758

References

Andrews, J.T., 2009. Seeking a Holocene drift ice proxy: non-clay mineral variations from the SW to N-central Iceland shelf: trends, regime shifts, and periodicities. J. Quat. Sci. 24, 664-676.

Aure, J., Strand, Ø., 2001. Hydrographic normals and long-term variations at fixed surface layer stations along the Norwegian coast from 1936 to 2000, Fisken og Havet 13, 1-24.

Belt, S.T., Allard, W.G., Massé, G., Robert, J.-M., Rowland, S.J., 2000. Highly branched isoprenoids (HBIs): Identification of the most common and abundant sedimentary isomers. Geochim.Cosmochim.Acta64, 3839-3851.

Belt, S.T., Brown, T.A., Navarro Rodriguez, A., Cabedo Sanz, P., Tonkin, A., Ingle, R., 2012.A reproducible method for the extraction, identification and quantification of the Arctic sea ice proxy IP_{25} from marine sediments.Analytical Methods 4, 705-713.

Belt, S.T., Brown, T.A., Ringrose, A.E., Cabedo-Sanz, P., Mundy, C.J., Gosselin, M., Poulin, M., 2013. Quantitative measurements of the sea ice diatom biomarker IP_{25} and sterols in Arctic sea ice and underlying sediments: Further considerations for palaeo sea ice reconstruction. Org. Geochem. 62, 33-45.

Belt, S.T., Massé, G., Rowland, S.J., Poulin, M., Michel, C., LeBlanc, B., 2007. A novel chemical fossil of palaeo sea ice: IP_{25}. Org. Geochem. 38**,** 16-27.

Belt, S.T., Massé, G., Vare, L.L., Rowland, S.J., Poulin, M., Sicre, M.-A., Sampei, M., Fortier, L., 2008. Distinctive ^{13}C isotopic signature distinguishes a novel sea ice biomarker in Arctic sediments and sediment traps. Mar. Chem. 112, 158-167.

Belt, S.T., Brown, T.A., Ringrose, A.E., Cabedo-Sanz, P., Mundy, C.J., Gosselin, M., Poulin, M., 2013. Quantitative measurements of the sea ice diatom biomarker IP_{25} and sterols in Arctic sea ice and underlying sediments: Further considerations for palaeo sea ice reconstruction. Org. Geochem. 62, 33–45.

Belt, S.T., Müller, J., 2013. The Arctic sea ice biomarker IP_{25}: a review of current understanding, recommendations for future research and applications in palaeo sea ice reconstructions. Quat. Sci. Rev. 79, 9-25.

Berben, S.M.P., 2014. A Holocene palaeoceanographic multi-proxy study on the variability of Atlantic water inflow and sea ice distribution along the pathway of Atlantic water.University of Tromsø (PhD thesis).

Berben, S.M.P., Husum, K., Cabedo-Sanz, P., Belt, S.T., 2014.Holocene sub-centennial evolution of Atlantic water inflow and sea ice distribution in the western Barents Sea, Clim. Past,10, 181-198.

Brown, T.A., Belt, S.T., Tatarek, A., Mundy, C.J., 2014. Source identification of the Arctic sea ice proxy IP_{25}.Nature Communications 5, 4197.

Cabedo-Sanz, P., Belt, S.T., Knies, J.K., Husum, K., 2013.Identification of contrasting seasonal sea ice conditions during the Younger Dryas.Quat. Sci. Rev. 79, 74-86.

Cabedo-Sanz, P., Belt, S.T., 2015.Identification and characterisation of a novel mono-unsaturated highly branched isoprenoid (HBI) alkene in ancient Arctic sediments. Org. Geochem. 81, 34-39.

Collins, L.G., Allen, C.S., Pike, J, Hodgson, D.A., Weckström, K., Massé, G. 2013. Evaluating highly branched isoprenoid (HBI) biomarkers as a novel Antarctic sea-ice proxy in deep ocean glacial age sediments.Quat. Sci. Rev. 79, 87-98.

de Vernal, A., Gersonde, R., Goosse, H., Seidenkrantz, M.-S., Wolff, E.W., 2013. Sea ice in the paleoclimate system: the challenge of reconstructing sea ice from proxies – an introduction. Quat. Sci. Rev. 79, 1-8.

Dickson, R., Rudels, B., Dye, S., Karcher, M., Meincke, J., Yashayaev, I., 2007. Current estimates of freshwater flux through Arctic and subarctic seas.Prog.Oceanogr. 73, 210-230.

Divine, D.V., Dick, D., 2006. Historical variability of sea ice edge position in the Nordic Seas.J. Geophys. Res. 111, C01001.

Ebbesen, H., Hald, M., 2004. Unstable Younger Dryas climate in the northeast North Atlantic. Geology 32, 673-676.

Fahl, K., Stein, R., 2012. Modern seasonal variability and deglacial/Holocene change of central Arctic Ocean sea-ice cover: New insights from biomarker proxy records. Earth Planet. Sci. Lett. 351–352, 123–133.

Hald, M., Andersson, C., Ebbesen, H., Jansen, E., Klitgaard-Kristensen, D., Risebrobakken, B., Salomonsen, G.R., Sarnthein, M., Sejrup, H.P., Telford, R.J., 2007. Variations in temperature and extent of Atlantic Water in the northern North Atlantic during the Holocene. Quat. Sci. Rev. 26, 3423-3440.

Hopkins, T. S., 1991. The GIN Sea: A synthesis of its physical oceanography and literature review, 1972-1985. Earth Sci. Rev. 30, 175-318.

Huang, W.Y., Meinschein W.G., 1976.Sterols as source indicators of organic material in sediments.Geochim.Cosmochim.Acta 40, 323–330.

Knies, J., 2005. Climate-induced changes in sedimentary regimes for organic matter supply on the continental shelf off northern Norway. Geochim. Cosmochim. Acta 69, 4631-4647.

Knies, J., Cabedo-Sanz, P., Belt, S.T., Baranwal, S., Fietz, S., Rosell-Melé, A., 2014. The emergence of modern sea ice cover in the Arctic Ocean. Nature Communications5, 5608.

Knies, J., Martinez, P., 2009. Organic matter sedimentation in the western Barents Sea region: Terrestrial and marine contribution based on isotopic composition and organic nitrogen content. Norwegian Journal of Geology 89, 79-89.

Kvingedal, B., 2005. Sea-ice extent and variability in the Nordic Seas, 1967-2002, in: Drange, H., Dokken, T., Furevik, T., Gerdes, R., and Berger, W. (Eds.): The Nordic seas: An integrated perspective, American Geophysical Union, Geophysical Monograph, 158, 39-49.

Loeng, H., 1991. Features of the physical oceanographic conditions of the Barents Sea, Polar Res., 10, 5-18.

Maiti, K., Carroll, J., Benitez-Nelson, C.R., 2010. Sedimentation and particle dynamics in the seasonal ice zone of the Barents Sea.J. Mar. Systems 79, 185-198.

Massé, G., Belt, S.T., Crosta, X., Schmidt, S., Snape, I., Thomas, D.N., Rowland, S.J., 2011. Highly branched isoprenoids as proxies for variable sea ice conditions in the Southern Ocean. Antarctic Sci.23, 487-498.

Massé, G., Rowland, S.J., Sicre, M.-A., Jacob, J., Jansen, E., Belt, S.T., 2008. Abrupt climate changes for Iceland during the last millennium: Evidence from high resolution sea ice reconstructions. Earth Planet. Sci. Lett. 269, 565-569.

Müller, J., Masse, G., Stein, R., Belt, S.T., 2009. Variability of sea-ice conditions in the Fram Strait over the past 30,000 years. Nature Geosci. 2, 772 – 776.

Müller, J., Wagner, A., Fahl, K., Stein, R., Prange, M., Lohmann, G., 2011.Towards quantitative sea ice reconstructions in the northern North Atlantic: A combined biomarker and numerical modelling approach. Earth Planet. Sci. Lett. 306, 137-148.

Müller, J., Werner, K., Stein, R., Fahl, K., Moros, M., Jansen, E., 2012. Holocene cooling culminates in sea ice oscillations in Fram Strait. Quat. Sci. Rev. 47, 1-14.

Müller, J., Stein, R., 2014. High-resolution record of late glacial sea ice changes in Fram Strait corroborates ice-ocean interactions during abrupt climate shifts. Earth Planet. Sci. Lett. 403, 446-455.

Navarro-Rodriguez, A., 2014. Reconstruction of recent and palaeo sea ice conditions in the Barents Sea. University of Plymouth (PhD thesis).

Navarro-Rodriguez, A., Belt, S.T., Brown, T.A., Knies, J., 2013.Mapping recent sea ice conditions in the Barents Sea using the proxy biomarker IP_{25}: implications for palaeo sea ice reconstructions.Quat. Sci. Rev. 79, 26-39.

Perette, M., Yool, A, Quartly, G.D., Popova, E.E., 2011. Near-ubiquity of ice-edge blooms in the Arctic. Biogeosciences 8, 515-524. Doi:10.5194/bg-8-515-2011.

Risebrobakken, B., T. Dokken, L.H. Smedsrud, C. Andersson, E. Jansen, M. Moros, Ivanova, E.V., 2011. Early Holocene temperature variability in

the Nordic Seas: The role of oceanic heat advection versus changes in orbital forcing, Paleoceanography 26, PA4206.

Rowland, S.J., Allard, W.G., Belt, S.T., Massé, G., Robert, J.-M., Blackburn, S., Frampton, D., Revill, A.T., Volkman, J.K., 2001.Factors influencing the distributions of polyunsaturated terpenoids in the diatom, *Rhizosoleniasetigera*.Phytochemistry 58, 717-728.

Rüther, D.C., Bjarnadóttir, L.J., Junttila, J., Husum, K., Rasmussen, T.L., Lucchi, R.G., Andreassen, K., 2012.Pattern and timing of the northwestern Barents Sea Ice Sheet deglaciation and indications of episodic Holocene deposition.BoreasDOI:10.1111/j.1502-3885.2011.00244.x.

Sakshaug, E., Johnsen, G., Kristiansen, S., von Quillfeldt, C., Rey, F., Slagstad, D., Thingstad, F., 2009. Phytoplankton and primary production, in: Sakshaug, E., Johnsen, G., Kovacs, K. (Eds), Ecosystem Barents Sea. Tapir Academic Press, Trondheim, pp.167-208.

Serreze, M., Barrett, A., Slater, A., Steele, M., Zhang, J., Trenberth, K., 2007.The large-scale energy budget of the Arctic.J. Geophys. Res., 112, D11122, doi.:10.1029/2006JD008230.

Stein, R., Fahl, K., 2013. Biomarker proxy IP_{25} shows potential for studying entire Quaternary Arctic sea-ice history. Org. Geochem. 55, 98-102.

Stoynova, V., Shanahan, T.M., Hughen, K.A., de Vernal, A., 2013. Insights into circum-Arctic sea ice variability from molecular geochemistry. Quat. Sci. Rev. 79, 63-73.

Stroeve, J.C., Serreze, M.C., Holland, M.M., Kay, J.E., Malanik, J., Barrett, A.P., 2012. The Arctic's rapidly shrinking sea ice cover: a research synthesis. Clim. Change. http://dx.doi.org/10.1007/s10584-011-0101-1.

Tolosa, L., Fiorini, S., Gasser, B., Martín, J., Miquel, J.C., 2013. Carbon sources in suspended particles and surface sediments from the Beaufort Sea revealed by molecular lipid biomarkers and compound-specific isotope analysis. Biogeosciences 10, 2061-2087. doi:10.5194/bg-10-2061-2013.

Vare, L.L., Massé, G., Gregory, T.R., Smart, C.W., Belt, S.T., 2009. Sea ice variations in the central Canadian Arctic Archipelago during the Holocene.Quat. Sci. Rev.28, 1354-1366.

Vare, L.L., Massé, G., Belt, S.T., 2010. A biomarker-based reconstruction of sea ice conditions for the Barents Sea in recent centuries. The Holocene, 40, 637-643.

Vinje, T.E., 1977. Sea ice conditions in the European sector of the marginal seas of the Arctic, 1966-75, Aarb. Nor. Polarinst. 1975, 163-174.

Volkman, J.K., 1986. A review of sterol markers for marine and terrigenous organic matter. Org. Geochem. 9, 83-99.

Wang, Y., Cheng, H., Lawrence Edwards, R., He, Y., Kong, X., An, Z., Wu, J., Kelly, M.J., Dykoski, C.A., Li, X., 2005. The Holocene Asian Monsoon: Links to solar changes and North Atlantic climate. Science 308, 854-857.

931 Xiao, X., Stein, R., Fahl, K., 2013. Biomarker distributions in surface
932 sediments from the Kara and Laptev Seas (Arctic Ocean): Indicators for
933 organic-carbon sources and sea ice coverage. Quat. Sci. Rev. 79, 40-52.

934 Xiao, X., Fahl, K., Müller, J., Stein, R., 2015. Sea-ice distribution in the
935 modern Arctic Ocean: Biomarker records from trans-Arctic Ocean surface
936 sediments. Geochim.Cosmochim.Acta155, 16–29.

937

938

939 **Figure Legends**

940

941 Figure 1. Structures of C_{25} highly branched isoprenoid (HBI) alkenes

942 described in the text. (I) IP_{25}; (II) $C_{25:2}$; (III) HBI III ($C_{25:3}$).

943

944 Figure 2. Mapsshowing the study region, major surface currents and sampling

945 locations. (a) Surface currents (Red – NAC: North Atlantic Current; NCaC:

946 North Cape Current; WSC: West Spitsbergen Current; Blue – ESC: East

947 Spitsbergen Current; BIC Bear Island Current); NCC: Norwegian Coastal

948 Current; (b) Locations of surface sediments (black circles) and long cores (red

949 circles). The positions of median April and September sea ice extent (1981–

950 2010; NSIDC) are also indicated.

951

952 Figure 3. Surface sediment concentrations of (a) IP_{25};(b) HBI III; (c)

953 brassicasterol. The positions of median April and September sea ice extent

954 (1981–2010; NSIDC), together with the maximum (1981) and minimum (2006)

955 April sea ice extent, are also indicated.

956

957 Figure 4.Downcorebiomarker concentration profiles of (a) IP_{25}; (b) HBI III; (c)

958 brassicasterol in core 70 obtained from the northern Barents Sea. IP_{25} and

959 brassicasterol data are taken from Berben (2014). PIP_{25} profiles based on HBI

960 III (d) and brassicasterol (e) are also shown, together with the respective *c*

961 factors. The diamonds on the x-axis denote the calibrated AMS ^{14}C

962 radiocarbon ages (Berben, 2014).

963

964 Figure 5. Downcore biomarker concentration profiles of (a) IP_{25}; (b) HBI III; (c)
965 brassicasterol in core 11 obtained from the western Barents Sea.Some of the
966 IP_{25} and brassicasterol data are taken from Berben et al. (2014). PIP_{25} profiles
967 based on HBI III (d) and brassicasterol (e) are also shown, together with the
968 respective *c* factors. The diamonds on the x-axis denote the calibrated AMS
969 ^{14}C radiocarbon (Berbenet al., 2014, Rüther et al., 2012).The shaded region
970 corresponds to the Younger Dryas (YD).
971
972 Figure 6. Downcore biomarker concentration profiles of (a) IP_{25}; (b) HBI III; (c)
973 brassicasterol in core 1200 obtained from the northern Norwegian Sea.IP_{25}
974 and brassicasterol data are taken from Cabedo-Sanz et al. (2013). PIP_{25}
975 profiles based on HBI III (d) and brassicasterol (e) are also shown, together
976 with the respective *c* factors. The diamonds on the x-axis denote the
977 calibrated AMS ^{14}C radiocarbon ages. The cross indicates the Vedde Ash
978 tephra horizon used in the age model (Cabedo-Sanz et al., 2013).The shaded
979 region corresponds to the Younger Dryas (YD).
980
981
982

Identification of paleo Arctic winter sea ice limits and the marginal ice zone: optimised biomarker-based reconstructions of late Quaternary Arctic sea ice.

Simon T Belt [a,*], Patricia Cabedo-Sanz [a], Lukas Smik [a], Alba Navarro-Rodriguez [a], Sarah M P Berben [b,1], Jochen Knies [c,d] and Katrine Husum [e]

Highlights

- Highly branched isoprenoid (HBI) biomarkers as Arctic sea ice proxies.
- Mono-unsaturated HBI (IP_{25}) characteristic of seasonal sea ice cover.
- Tri-unsaturated HBI (HBI III) enhanced within the Marginal Ice Zone (MIZ).
- Combination of IP_{25} and HBI III improves descriptions of sea ice conditions
- Novel proxy method applied successfully in Holocene and Younger Dryas records

[1] Current Address: Department of Earth Science and the Bjerknes Centre for Climate Research, University of Bergen, N-5007 Bergen, Norway.

Figure

Click here to download Figure: Figure 1.docx

Figure 1

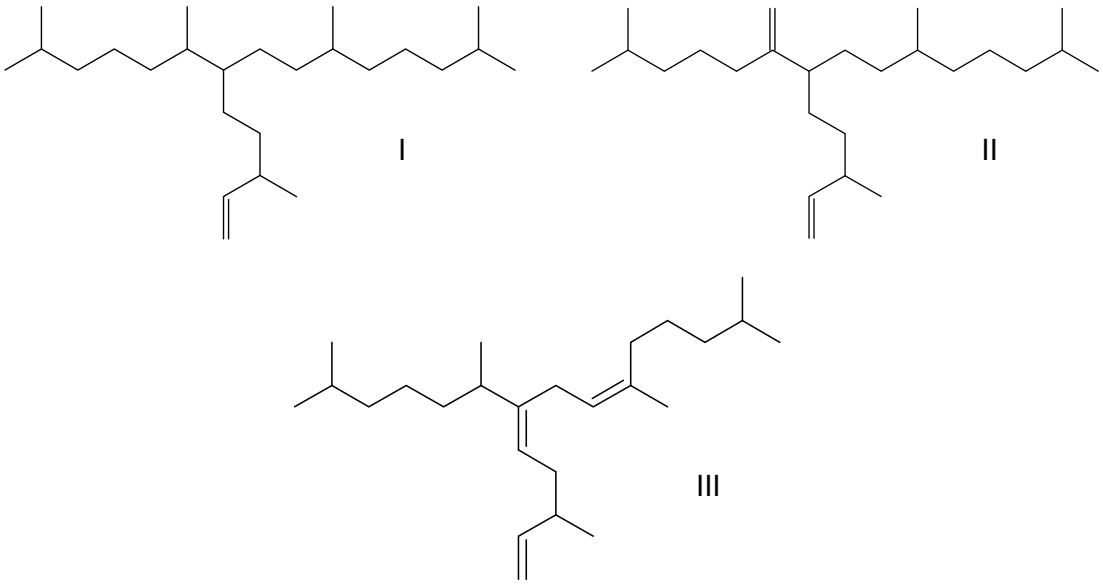

Figure

Click here to download Figure: Figure 2.docx

Figure 2

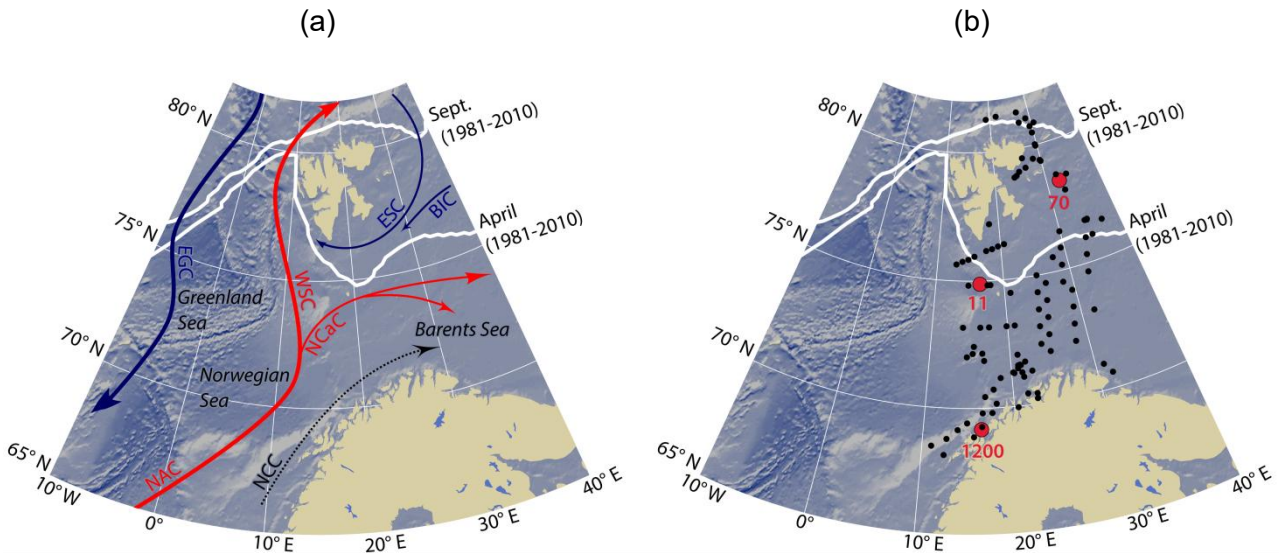

Figure

Click here to download Figure: Figure 3.docx

Figure 3

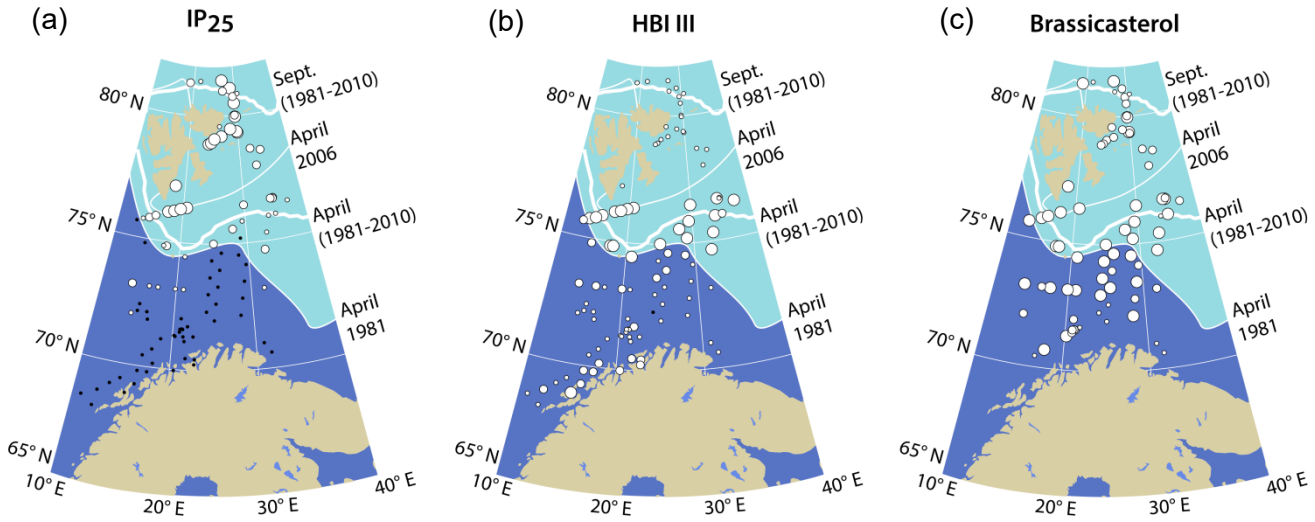

Biomarker concentrations (ng g^{-1})			
	IP_{25}	HBI III	Brassicasterol
·	0	0	0
◦	<2	<2	<200
○	2-5	2-5	200-500
○	>5	>5	>500

Figure

Click here to download Figure: Figure 4_revised.docx

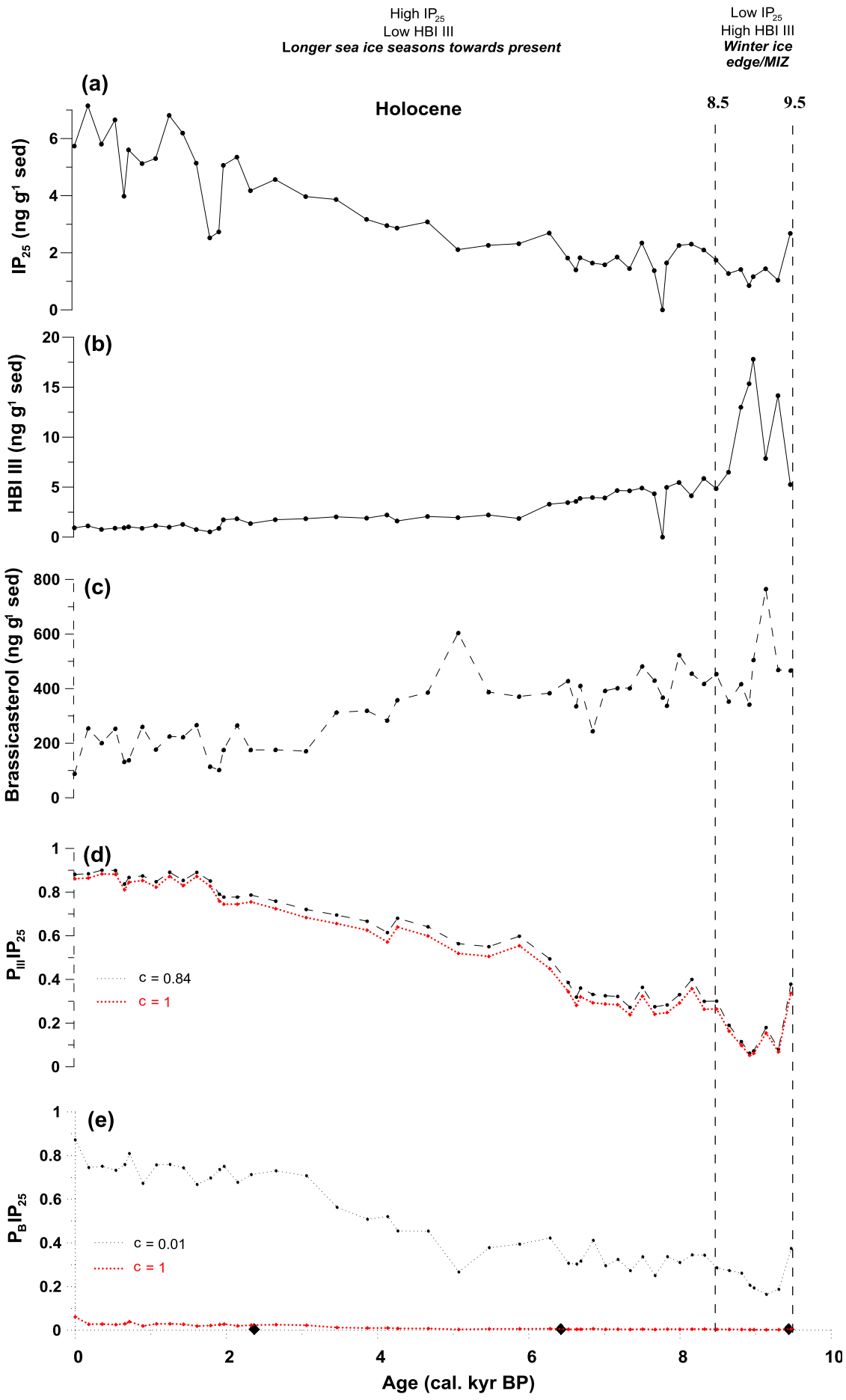

Figure

Click here to download Figure: Figure 5_revised.docx

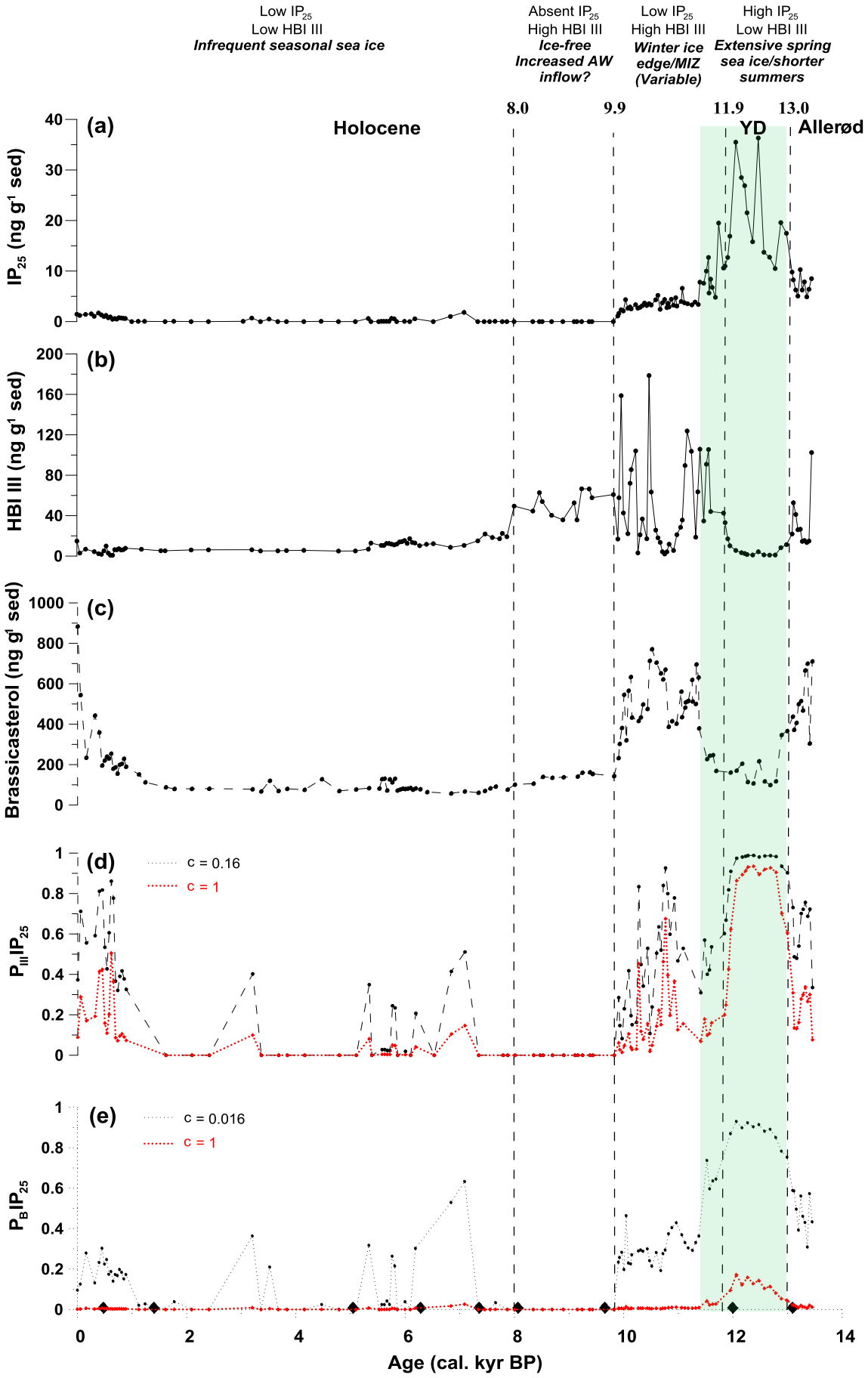

Figure

Click here to download Figure: Figure 6_revised.docx

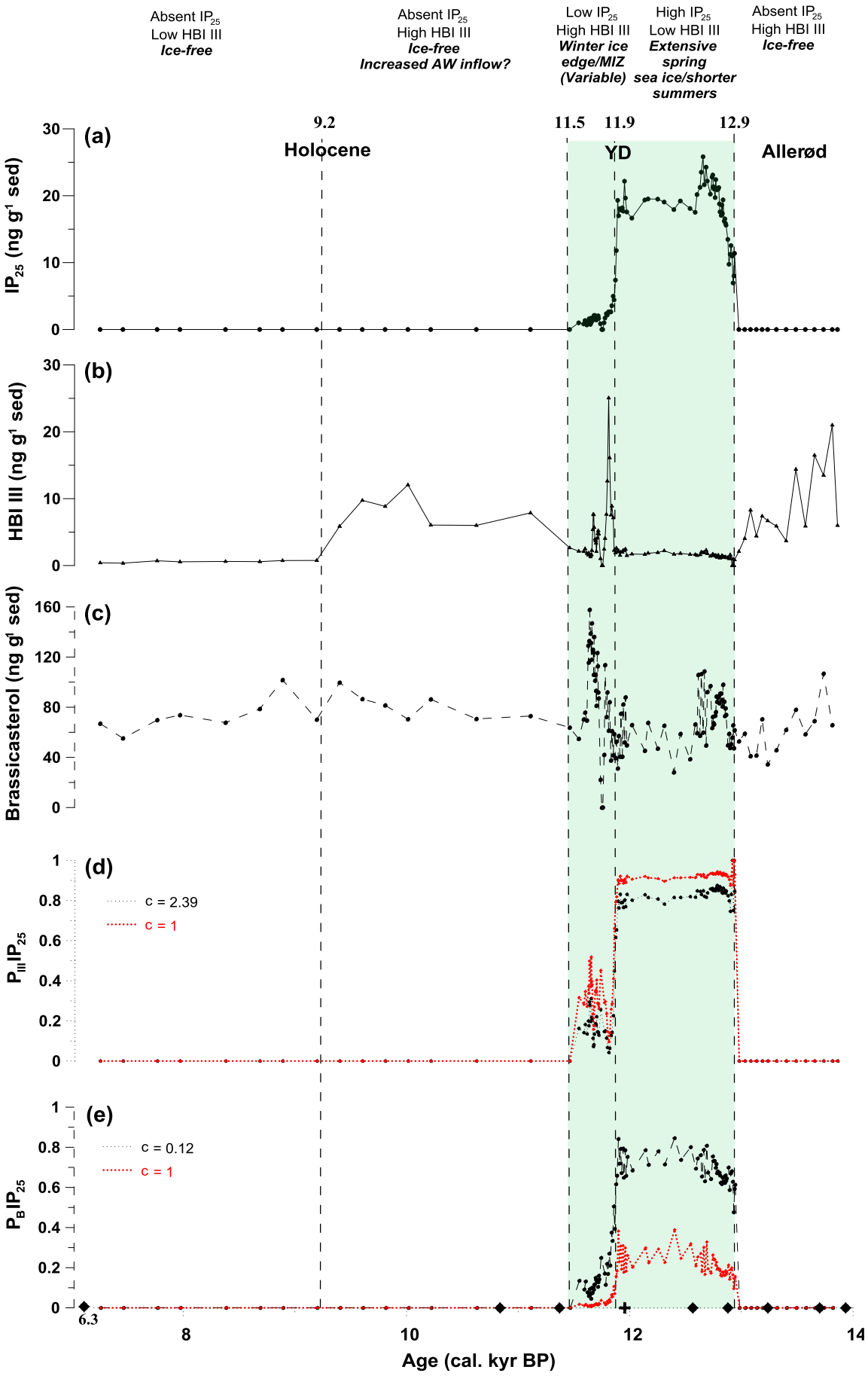

Supplementary material for online publication only

Click here to download Supplementary material for online publication only: Supplementary Table 1_revised.docx